Design of a Defective Grounded Monopole Patch Antenna with Slotted Book-Shaped Patch Structure for Microwave-Based Imaging Applications

Sarna Majumder[1*], Md Siam Talukder[2], Naimur Rahman[3]
Abdul Masud[4], Md. Samsuzzaman[1]

[1]Department of Computer and Communication Engineering, Patuakhali Science and Technology University, Dumki Patuakhali-8602, Bangladesh
[2]Faculty of Computer Science and Engineering, Patuakhali Science and Technology University, Dumki, Patuakhali-8602, Bangladesh
[3]Department of Electrical and Electronics Engineering, Patuakhali Science and Technology University, Dumki Patuakhali-8602, Bangladesh
[4]Department of Computer Science and Information Technology, Patuakhali Science and Technology University Dumki, Patuakhali-8602, Bangladesh
*Correspondence: E-mail: sarna.cse@pstu.ac.bd
(Received Date: 23 August 2022, Accepted Date: 22 September 2022)

Abstract: In this article, a novel Book-Shaped Rectangular Slotted Patch with a Defected Ground Antenna has been developed for microwave-based imaging purposes. Its design consists of a rectangular slotted book-shape patch structure and a defective ground plane. The antenna design is capable of exhibiting multi-resonances and revealing the spectrum in a wideband manner. As a whole, it measures $0.26\lambda \times 0.17\lambda \times 0.007\lambda$ (where λ is the wavelength at the lower frequency of 1.41 GHz). The experimental data shows that the antenna operates effectively between 1.41 and 2.52 GHz (<-10 dB) with an FBW of 57%. The designed antenna has a maximum gain of 3.6 dBi at 2.51 GHz as determined by simulation results. The CST simulation results are consistent enough with the experimental data. This antenna is ideal for use in biomedical imaging because of its small size, sufficient gain, wide operating band, high efficiency, and consistent omnidirectional radiation properties.

Keywords: Biomedical imaging, defective grounded monopole antenna, microwave-based imaging, multi-resonances, rectangular slotted patch.

Introduction

In case of any clinical analysis and medical intervention, better understanding of the internal part of a human body is required. Medical imaging is the technique to accomplish this by creating visual representations of the human's internal organs and tissues. There are various types of medical imaging technologies like magnetic resonance imaging (MRI), ultrasound, endoscopy, CT and even, nuclear medical imaging. We know that MRI and ultrasound are very much operator dependent and costly. Over the past few years several attempts have been made by the scientists to find better alternative solutions. One such popular solution is using microwave medical imaging techniques. This technique is preferred over other methods for a variety of reasons. The main reason can be it's non-invasive nature i.e. it does not require any kind of surgery. It is also safer than X-rays, since it is a non-ionizing method. In addition to this, microwave imaging technique gives immediate results and is highly sensitive in detecting cancerous tumours (Wang, 2014). This technique offers more distinct electrical contrast between cancerous tumours and healthy tissue, lower power radio frequency signals and low health risks and more comfort to the patient (De Zaeytijd et al., 2007). The cost and complexity for developing a microwave imaging system could be far less than that for MRI

and CT due to the extensive use of microwaves over the world especially in telecommunications. In 2013, Wang and Simpkin have shown that microwave imaging can be developed as a detector for 'perfusion related changes in the brain' and used for 'imaging modality for stroke management'.

Specifically, in this study, we attempted to improve brain tumor detection systems by developing and fabricating a single-layered compact planar monopole antenna. The top radiator is fed by a 50Ω line with a grounded back reflector. The top radiator in the side position with defective ground enhances overall directivity. In comparison to the existing literature, this led to a reasonable tradeoff between antenna dimension and directivity. Along with its small size, the antenna is developed and manufactured on a low-cost FR-4 substrate with dielectric characteristics of 4.3 and a loss tangent of 0.003. This substrate ensures cost-effectiveness and provides greater accessibility to brain tumor detection because it is readily available. The antenna proposed for use from 1.41 GHz to 2.52 GHz can operate with a reasonable agreement between simulation and measurement, with a stable radiation pattern, improved directivity, and a decent gain of 3.6 dBi.

Due to the lack of access to clinical imaging, researchers are conducting intensive research to identify brain tumors early (Chandra et al., 2015). Antennas worn as part of clothing, or attachable to the human body, are electronic devices that can be worn on a regular basis. Nevertheless, designing such antennas is a challenging endeavor, since electromagnetic interactions between the body and the antenna strongly affect their performance (Rokunuzzaman et al., 2016) . Screening tumors can include several procedures, including X-rays, MRIs, CT-scan and biopsies. However, when used regularly, these techniques may induce mental anguish in patients and emit hazardous ionizing radiation (Hossain and Mohan 2017). Furthermore, this equipment requires a highly trained physician to operate and is very expensive to maintain. In addition to this, these technologies have low accuracy rates/false-positive rates ranging from 60 to 70 %. The microwave imaging method (MWI) is another approach for detecting early brain tumors. In addition to its low cost as it requires little investment in hardware, ease of use, non-invasive nature, mobility, and efficiency, such a technique is advantageous for the detection and localization of tumors (Bashri and Arslan 2018; Casu et al., 2017).

When using microwave imaging, the antenna is one of the most important components. A range of microwave brain imaging techniques has been developed in recent years using a variety of antennas. When an antenna operates in the lower-frequency band, it offers deep penetration, while antennas that operate in the higher-frequency band offer a better resolution (Alani et al., 2020). In the year of 2017, Abbak et al. has utilized a Vivaldi antenna to provide a high gain as well as wider bandwidth. Such qualities were obtained by expanding the number of curvatures and the antenna dimension at the same time. Some squared monopole antennas were utilized for MWI in addition to Vivaldi antennas because of their broad bandwidth and manufacturability (Ahadi et al., 2015). However, in 2015, Ojaroudi ansd Ghadimi included custom-designed slots into the antenna bottom radiator (defected ground plane) to enable a broad working bandwidth. Furthermore, the monopole antenna suggested by Bah et al. in 2015, had L-shaped slots in the back radiator to increase bandwidth. The ground plane was modified with a two-slot geometric design (T-shaped and E-shaped slots/strips) to achieve more than 86% radiation efficiency over the functional range (Ojaroudi et al., 2012). In 2018, Subramanian et al. have presented an ultra-wideband (UWB) monopole antenna that

operates over a wide frequency range, with an octagonal-shaped patch to optimize radiation efficiency. Printed Monopole antennas are usually flexible and easy to fabricate, and they are also largely affordable, compact, lightweight, and low-cost (Ojaroudi and Ghadimi, 2015; Talukder et al., 2022). Moreover, they have a proclivity for producing bidirectional radiation (Li et al., 2020). Besides, for the purposes of the wireless communication system, a printed monopole antenna has been described in reference (Azim et al. 2022). This antenna was able to obtain a decent bandwidth of 1.78 GHz (2.02 -3.8 GHz) and has the capability to cover narrow bands such as ISM, IMT, Wi-Fi, Bluetooth, WiMAX, and WLAN.

Microwave imaging is indeed a new tool for detecting early brain tumors detection. This has been recommended as a reliable, portable, and cost-effective supplement to traditional imaging technologies. The MWI hardware installation system's cheap cost and mobility make it excellent for application in coastal locations. The antenna that delivers microwaves and collects backscattered impulses from the irradiated objects determines the functionality of a microwave-based imaging hardware system (Mahmud et al., 2018). An improved image resolution can be achieved through the use of a higher frequency, but at a cost of shorter wavelengths and lesser penetration depths, making it unable to identify small, deep-lying malignancy. In spite of the lack of consensus on what bandwidth is best suited to MWI, spectrum optimizations for the MWI system for tissue sensing remain a topic of investigation. Bahramiabarghouei et al. (2015) nonetheless obtained optimal findings between 2GHz and 4GHz. Again, for the detection of malignancy, a monopole antenna has been proposed in (Alam et al. 2022). The developed prototype offers omnidirectional radiation capabilities in addition to a bandwidth of 1.12 GHz (1.40-2.52 GHz). However, this prototype exhibits a gain that is quite modest over the active frequency range. In (Talukder et al. 2021), a printed monopole antenna is reported for use in tumor detection. This design offers a bandwidth of 2.37 GHz, as well as 100% of the fractional bandwidths (% BW), all while maintaining a reflection coefficient of < -10 dB. However, the total size of the antenna, which measures 70 × 60 × 1.5 mm3, is not considered to be tiny. In spite of the fact that the antenna was able to exhibit high gain and good microwave signal penetration for brain tumor diagnostics, the proposed antenna size was very large.

Authors in this study have attempted to develop and fabricate a single-layered compact planar monopole antenna which will improve present brain tumor detection systems. The next section will present the antenna design procedure. In addition to the simulations and parametric study, it also provides experimental results. The last section concludes with some final remarks.

Materials and Methods

Figure 1. depicts a schematic depiction of the proposed wideband monopole antenna, along with design development processes. CST Microwave Studio is used to simulate and design this device, and FR-4 material is used as its substrate (dielectric constant, ϵ_r = 4.4, and loss tangent, tan δ = 0.02). As included in Figure 1, there are three main key phases in the antenna design process (Design 1 through Design 3). Antenna design has been developed beginning with a full ground plane and open-book shape patch structure. To finalize the designed ground and patch shape, various parameters were examined with parametric analysis and also by using a try-and-error method. A simple, unslotted, open book shaped patch is developed as the top radiator on the top layer with a complete ground plane of Design 1 for the initial phase.

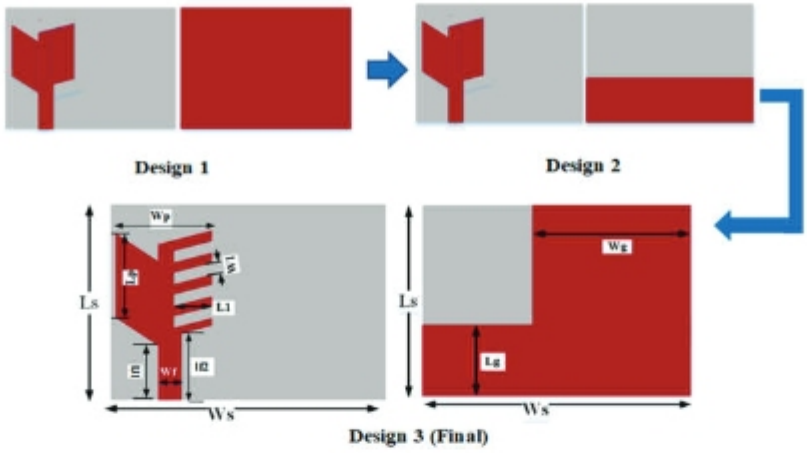

Figure 1. Design Evolution Steps and Final Antenna Design with Precise Measurements.

Next, the bottom complete ground plane radiator is trimmed and converted into a partial ground plane (Design 2). This trimmed ground plane affects energy conservation in substrates, hence reducing the quality factor (Q). A third stage entails modifying the patch and ground plane of Design 2 in order to improve impedance bandwidth, resulting in Design 3, shown in Figure 1. Multiple rectangular slots, like steps on a stairway, are incorporated at this phase into the top patch radiator. This approach resulted in an improvement to the antenna impedance matching throughout a broad frequency range (Al-Gburi et al., 2019).

In terms of overall size, the antenna (with substrate) measure 37 mm in length (*Ls*) and 56 mm in width (*Ws*). The microstrip line that supplies the main patch has dimensions of 13.50 mm and 16 mm for its length (*Lf1*, *Lf2*) and 3.0 mm for its width (*Wf*), and it is terminated via a wave-guide port for simulation. Meanwhile, the patch radiator has an overall size that is calculated as 14×16 mm^2 (length, *Lp* × width, *Wp*). The patch radiator has identical dimensions on both wings (left and right). To the right wing, there have been four symmetrical rectangular slots of 6 mm in length (*L1*) and 2 mm in width (*W1*).

Table 1 below summarizes the relevant optimized antenna dimensions.

Table 1. Overall relevant optimized antenna parameters dimensions.

Parameters	Description	Value (mm)
Ls	Substrate length	37
Ws	Substrate width	56
Sh	Substrate thickness	1.60
Lp	Patch length	14
Wp	Patch width	16
mt	Metal thickness	0.03
Lf1	Feed line length 1	13.50
Lf2	Feed line length 2	16.00
Wf	Feed line width	3
Lg	Ground length	12.50
Wg	Ground width	32.50
L1	Patch slot length	6
W1	Patch slot width	2

Results and Discussion

Simulated Results

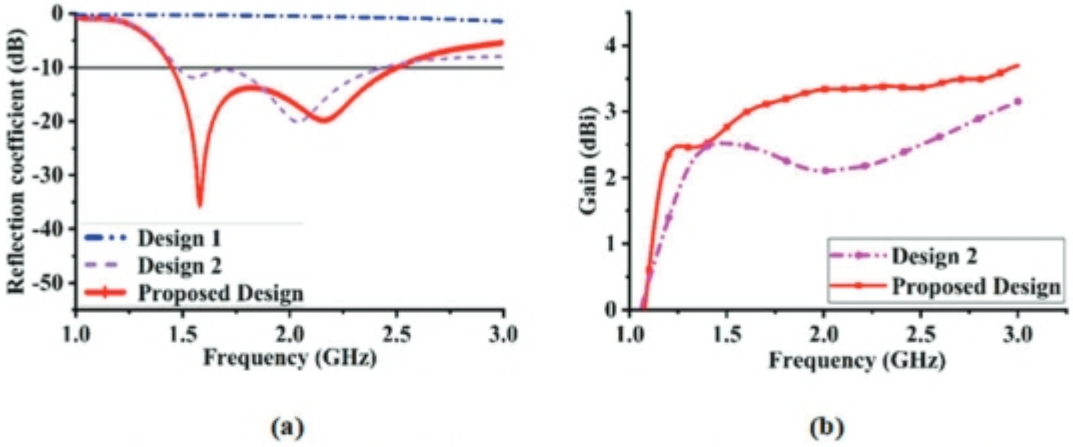

Figure 2. Antenna Performance in Each Step of Try and Error Method; (**a**) Reflection Coefficient; (**b**) Gain.

Figure 2 depicts the reflection coefficients (S_{11}), resonant frequencies and gain at several phases of the design, including Design 1, Design 2, and Proposed Design. Overall summary of antenna performance during the design evolution process is compiled in Table 2. The change in geometry is the primary cause of the fluctuation in operating frequency that occurs between the various stages of design. Figure 1 demonstrates that the design process begins with a full ground plane, which is the primary cause of the failure to provide more reactance, which is an essential requirement for the wideband responses. When the ground plane is completely filled in, there is a rise in the amount of conserving energy in the substrate; as a result, there is no effective bandwidth that is lower than 10 dB. Thus, for further progression, instead of a full reflecting surface on the rare side of the antenna, a partial ground plane has been chosen. This alteration leads to a wideband response because it provides extra reactance and lowers the amount of energy that can be conserved in the substrate.

Table 2. Summary of Antenna Performance during the Design Evolution Process.

Design	Resonant frequency (GHz)	Reflection coefficient level (dB)	Frequency range and Bandwidth (GHz)	Gain (dBi)
Design-1	No Band	No Band	No Band	N/A
Design-2	2.1 GHz	20 dB	1.41 – 2.50	2.5
Proposed Design	1.58 GHz and 2.17 GHz	36 dB	1.41 – 2.52	3.6

Design 2 is capable of functioning in a broad frequency range, which extends from 1.41 GHz to 2.50 GHz (55 percent of fractional bandwidth). However, at 1.7 GHz, Design 2 exhibits a very poor reflection coefficient that is extremely near to the reference level of -10 dB. In addition, over the operational frequency range, this structure generates only one resonance mode below-20 dB at 2.1 GHz. The final design incorporates additional rectangular slots on the patch radiator and an expanded ground structure. As compared to Design 2, this antenna

had an improved bandwidth and minimum reflection coefficient. According to its reflection coefficient characteristic, this antenna produces resonant at the lower frequency and combines multiple wideband resonant mode at 1.58 GHz and 2.17 GHz. In Figure 2(b), antenna gains are shown at each stage of the design evolution. Since the first phase generates no useful bandwidth, the gain of this stage is disregarded. With the development of the design, the antenna demonstrates better gain. The antenna achieves its maximum gain of 2.5 dBi at a frequency of 2.49 GHz during the second phase, which reaches almost 3.6 dBi at the final modification with a multiple-slotted structured patch.

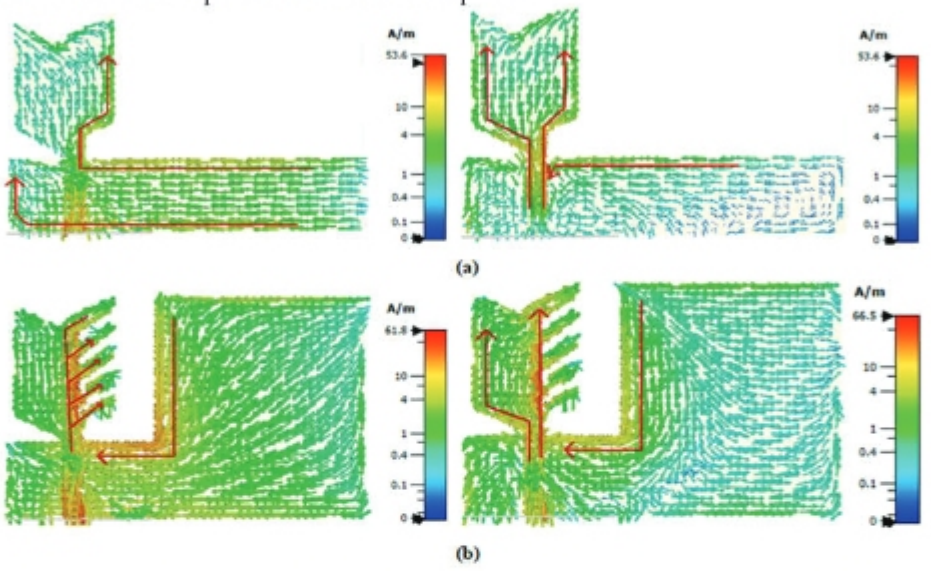

Figure 3. Surface current allocation for different step of design evolution at multiple frequency point; (a) Design 2 at 1.58 GHz and 2.17 GHz, (b) Final design at 1.58 GHz and 2.17 GHz.

A complete ground plane and an unslotted patch radiator were the initial components of the proposed antenna design. Then, we conducted parametric research to evaluate several parameters, and the trial-and-error approach to settle on the proposed ground and patch form. For each stage of design evolution, we can readily explain how surface current impacts antenna bandwidth and resonance frequency by surface current analysis. For the surface current analysis, conventional design with a complete ground structure generates no effective bandwidth lower than -10 dB, thus we disregard the early phase. The surface current distribution at two distinct frequencies is shown in Figure 3, for both Design 1 and the proposed design. Figures 3(a) and 3(b) illustrate surface currents at 1.58 GHz and 2.17 GHz for design 1 and the Proposed design, respectively.

In patch antennas, the ground plane as a radiator actually experiences a reverse current in the bottom. Therefore, by adding a slot(s) exactly below the antenna's radiating patch, the surface current on the ground is forced to loop around the slot (Yoon et al., 2021). Due to the rotating surface currents in the radiation element, additional polarization is generated via ground plane slots which in turn affects the power flow. Consequently, antenna performance was enhanced in regards to the bandwidth and polarization of the radiation pattern. As illustrated in Figures 3(a) and 3(b), the reversed current on the ground plane greatly impacts lower frequencies for design 1 as well as lower resonance at 1.58 GHz for the proposed design.

In design 2, the maximum surface current is dispersed throughout the patch radiator at a higher frequency of 2.17 GHz. There are many rectangular slots that could be employed in the proposed design to divert surface current away from its usual path. For higher resonance at 2.17 GHz, this patch current has a significant influence. At resonance frequencies of 1.58 GHz and 2.17 GHz for the proposed design, as seen in Figure 3(b), the slotted patch radiator and its adjacent regions on ground, the slotted bottom edge and right edge have substantially higher current densities than the rest of the antenna portion. Due to its quarter-wave resonant properties, this region of ground is a significant contributor to maximum current production. The length of the current path in this instance, also known as the resonant length, is (1)

$$l_{fr} = \frac{\lambda}{4} \qquad (1)$$

Here, λ corresponds to the wavelength of fundamental resonances in free space.

Experimental Outcomes

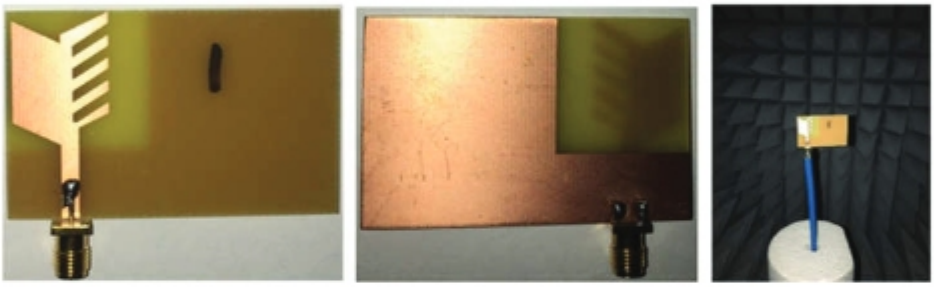

Figure 4. Fabricated Prototype and Anechoic Chamber Measurement.

Figure 4 illustrates the fabricated prototype, for which optimal parameter values were used in its fabrication. Reflection coefficients (dB) of the prototype are determined using the PNA Network analyzer. The frequency range that the PNA can operate in ranges from 10 MHz up to 67 GHz. Experimental radiation patterns are assessed in anechoic chambers as depicted in Figure 4. As can be shown in Figure 5(a), the impedance bandwidth (IBW) of the fabricated prototype is between 1.41 GHz to 2.52 GHz, and the reflection coefficient is below-20 dB at its minimum level. According to the results of the experiments, the FBW is up to 57 %. Similar to the simulated result, the measured result also produces two resonance frequencies. In Figure 5(b), the measured gain through Satimo Starlab is compared to simulated gain (CST).Simulation results show a maximum gain of approximately 3.6 dBi and an average gain of 3.12 dBi.The fabricated prototype, however, was measured to have a maximum gain of 4 dBi at a frequency of 1.5 GHz based on the measured results.Therefore, the designed antenna has a comparatively light structure while providing superior gain compared with other proven head-imaging antennas. A comparison of the simulated and experimental efficiencies can be seen in Figure 5(c).According to the simulated results of the antenna, the antenna has an efficiency of more than 95%.However, the impacts that were assessed show some degree of variance in this particular instance.The efficiency of the fabricated prototype is more than 80%.Tolerances in the fabrication and welding processes might be responsible for the minuscule mismatch between the simulated and actual results.The outcomes of these measurements, however, are suitable for use in imaging applications. Both simulated and experimental co- and cross-polarization radiation patterns in XZ and YZ plane are presented in Figures 5(d) and 5(e) for the most significant resonant frequency, 1.58 GHz.

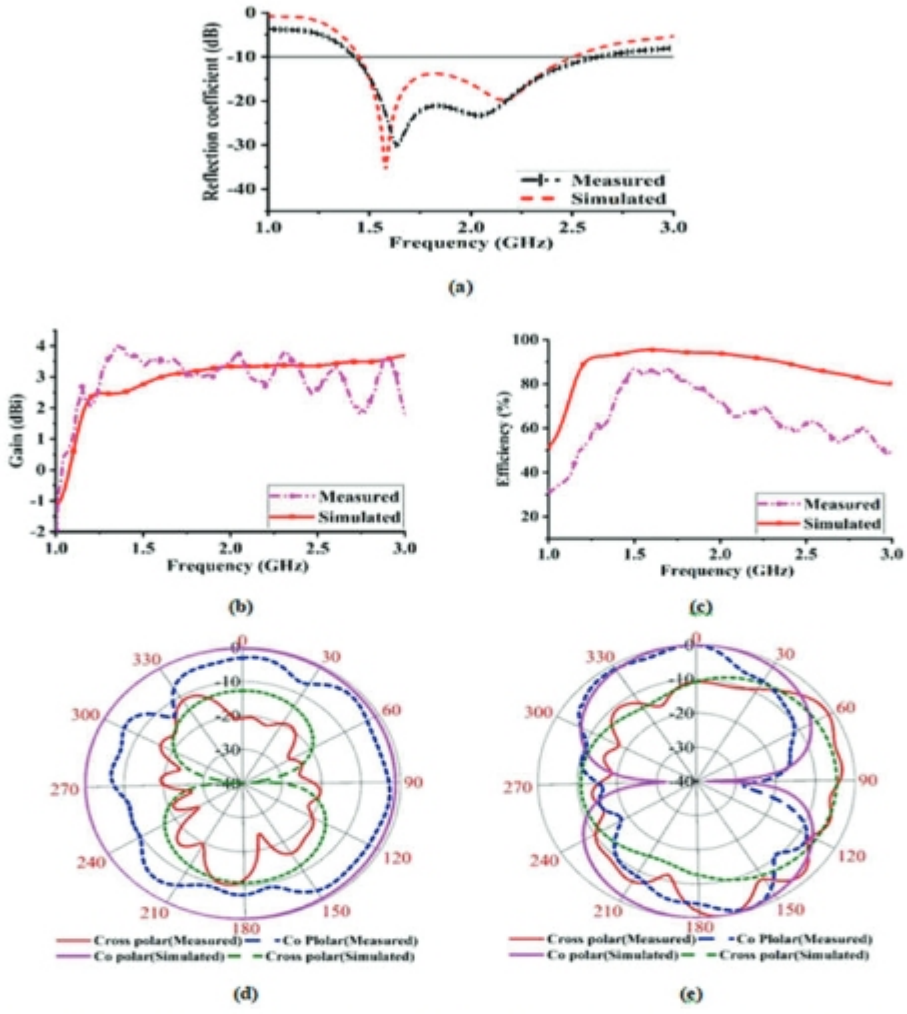

Figure 5. Measured antenna properties; (**a**) Reflection coefficient, (**b**) max gain(dBi), (**c**) radiation efficiency (%), (**d**) radiation pattern at 1.58 GHz alongxz-plane, **(e)** radiation pattern at 1.58 GHz alongyz-plane.

The figure clearly demonstrates that the radiation pattern emitted by the antenna remains symmetrical regardless of the frequency at which it is operating. When it comes to biomedical-related microwave systems, using antennas that emit in an asymmetrical pattern offers a number of major advantages. For example, the maximum power is being emitted in the bore-view directions, i.e., in the intended region, and doesn't shift to another direction at other frequencies, ensuring constant electrical field distributions. As a second benefit, if this single antenna element is employed to build an array arrangement, the radiation pattern remains constant across the operating range. Furthermore, it can be shown that this antenna has a negligible amount of cross-polarization. Finally, the designed prototype is compared in Table 3 to several proven antenna designs for MWI applications. The new antenna has the advantages of being more compact, having a larger frequency range, and having a far greater gain than previous antennas.

Table 3. Performance Comparison with Some Earlier Antennas.

Ref.	Dimension	Substrate	Substrate Layer	IBW (GHz)	FBW (%)	Gain (dBi)	Application
(Salleh et al., 2019)	50×60×1.5 mm^3	Rogers RO4350B	1	2.06-2.61	23.55%	2.45	Head imaging
(Alqadami et al., 2018)	85×60×4.0 mm^3	PDMS	5	1.16-1.94	53.8%	NR	Head imaging
(Hasan et al., 2020)	56×37×1.6 mm^3	FR-4	1	1.45-2.52	53.90%	2.4	Head imaging
(Nesar et al., 2018)	29.99×29.99 ×0.59 mm^3	FR-4	1	0.6-1.3	73.68%	<3	Head imaging
(Hossain et al., 2020)	50×44×1.52 mm^3	Rogers RO4350B	1	1.70-2.71	52.3%	>3.5	Head imaging
(Sohani et al., 2020)	79×68.28 mm^2	FR-4	1	1-2	10%	NR	Head imaging
(Alam et al., 2022)	37×56×1.6 mm^3	FR-4	1	1.4 - 2.5	55%	3.5	Head imaging
(Talukder et al., 2021)	70× 60× 1.5 mm^3	FR-4	1	1.19 - 3.56	100%	5.9	Head imaging
(Azim et al., 2022)	NR	Rogers RO4350B	1	2.02 - 3.8	61%	<4	Wireless communi-cation
(Merunka et al., 2019)	59×59×1.5 mm^3	FR-4	2	0.9-1.3	36.36%	3.10	Head imaging
Proposed	37×56×1.5 mm^3	FR-4	1	1.41 - 2.52	57 %	≈ 4	Head imaging

Conclusions

This research proposes a rectangular slotted patch with a defective grounded monopole patch antenna for microwave-based object (tumor) recognition in biomedical imaging. The proposed antenna excels in various respects: its fractional bandwidth (FBW) is 57 %, and its gain is greater than 3.6 dBi. Furthermore, the acquired bandwidth spans from 1.41 GHz to 2.52 GHz, which is perfect since low-frequency electromagnetic radiation may go deeper into tissues with less attenuation. The finalized measurements were 56×37×1.6 mm^3. In order to test how well the antenna design would work in practice, FR4 substrate prototypes were made and tested in the lab. When the results of the simulation are compared to the actual results, there is a decent amount of consistency. With its steady omnidirectional radiating capabilities, the designed antenna can be implanted in the desired location either facing forward or backward.

Funding: This research was funded by Patuakhali Science and Technology University Research Grant, Code: **PSTU/RTC-B/01/15/26(59)**.

Acknowledgments: This work is supported by the Patuakhali Science and Technology University Research Grant. The technical support required for experiment was provided by the Microwave lab, UKM, Malaysia.

Conflicts of Interest: The authors declare no conflict of interest.

References

Abbak, M., Akıncı, M.N., Çayören, M. and Akduman, İ., 2017. Experimental microwave imaging with a novel corrugated Vivaldi antenna. *IEEE Transactions on antennas and propagation*, *65*(6), pp.3302-3307.

Ahadi, M., Isa, M.B.M., Saripan, M.I.B. and Hasan, W.Z.W., 2015. Square monopole antenna for microwave imaging, design and characterisation. *IET Microwaves, Antennas & Propagation*, *9*(1), pp.49-57.

Alam, M.M., Talukder, M.S., Samsuzzaman, M., Khan, A.I., Kasim, N., Mehedi, I.M. and Azim, R., 2022. W-shaped slot-loaded U-shaped low SAR patch antenna for microwave-based malignant tissue detection system. *Chinese Journal of Physics*, *77*, pp.233-249.

Alani, S., Zakaria, Z. and Ahmad, A., 2020. Miniaturized UWB elliptical patch antenna for skin cancer diagnosis imaging. *International Journal of Electrical & Computer Engineering (2088-8708)*, *10*(2).

Alqadami, A.S., Bialkowski, K.S., Mobashsher, A.T. and Abbosh, A.M., 2018. Wearable electromagnetic head imaging system using flexible wideband antenna array based on polymer technology for brain stroke diagnosis. *IEEE transactions on biomedical circuits and systems*, *13*(1), pp.124-134.

Al-Gburi, A.J.A., Ibrahim, I., Zakaria, Z. and Khaleel, A.D., 2019. Bandwidth and gain enhancement of ultra-wideband monopole antenna using MEBG structure. *Journal of Engineering and Applied Sciences*, *14*(10), pp.3390-3393.

Azim, R., Dhar, K., Mia, M.S. and Islam, M.T., 2022. Inset-fed microstrip patch antenna for ubiquitous wireless communication applications. *International Journal of Ultra Wideband Communications and Systems*, *5*(2), pp.57-64.

Bah, M.H., Hong, J. and Jamro, D.A., 2015. Ground slotted monopole antenna design for microwave breast cancer detection based on time reversal MUSIC. *Progress In Electromagnetics Research C*, *59*, pp.117-126.

Bahramiabarghouei, H., Porter, E., Santorelli, A., Gosselin, B., Popović, M. and Rusch, L.A., 2015. Flexible 16 antenna array for microwave breast cancer detection. *IEEE Transactions on Biomedical Engineering*, *62*(10), pp.2516-2525.

Bashri, M.S.R. and Arslan, T., 2018. Low-cost and compact RF switching system for wearable microwave head imaging with performance verification on artificial head phantom. *IET Microwaves, Antennas & Propagation*, *12*(5), pp.706-711.

Casu, M.R., Vacca, M., Tobon, J.A., Pulimeno, A., Sarwar, I., Solimene, R. and Vipiana, F., 2017. A COTS-based microwave imaging system for breast-cancer detection. *IEEE transactions on biomedical circuits and systems*, *11*(4), pp.804-814.

Chandra, R., Zhou, H., Balasingham, I. and Narayanan, R.M., 2015. On the opportunities and challenges in microwave medical sensing and imaging. *IEEE transactions on biomedical engineering*, *62*(7), pp.1667-1682.

De Zaeytijd, J., Franchois, A., Eyraud, C. and Geffrin, J.M., 2007. Full-wave three-dimensional microwave imaging with a regularized Gauss–Newton method—Theory and experiment. *IEEE Transactions on Antennas and Propagation*, *55*(11), pp.3279-3292.

Hasan, M.M., Samsuzzaman, M., Talukder, M.S., Islam, M.T., Azim, R. and Masud, M.A., 2020, December. Wideband slotted patch antenna for microwave based head imaging applications. In *2020 2nd International Conference on Sustainable Technologies for Industry 4.0 (STI)* (pp. 1-4). IEEE.

Hossain, A., Islam, M.T., Chowdhury, M.E. and Samsuzzaman, M., 2020. A grounded coplanar waveguide-based slotted inverted delta-shaped wideband antenna for microwave head imaging. *IEEE Access*, *8*, pp.185698-185724.

Hossain, M.D. and Mohan, A.S., 2017. Cancer detection in highly dense breasts using coherently focused time-reversal microwave imaging. *IEEE Transactions on Computational Imaging*, *3*(4), pp.928-939.

Li, N.Y., Zakaria, Z., Shairi, N.A., Alsariera, H. and Alahnomi, R., 2020. Design and investigation on wideband antenna based on polydimethylsiloxane (PDMS) for medical imaging application. *no*, *3*, pp.89-92.

Mahmud, M.Z., Islam, M.T., Misran, N., Almutairi, A.F. and Cho, M., 2018. Ultra-wideband (UWB) antenna sensor based microwave breast imaging: A review. *Sensors*, *18*(9), p.2951.

Merunka, I., Massa, A., Vrba, D., Fiser, O., Salucci, M. and Vrba, J., 2019. Microwave tomography system for methodical testing of human brain stroke detection approaches. *International Journal of Antennas and Propagation*, *2019*.

Nesar, M.S.B., Chakma, N., Muktadir, M.A. and Biswas, A., 2018, October. Design of a miniaturized slotted T-shaped microstrip patch antenna to detect and localize brain tumor. In *2018 International Conference on Innovations in Science, Engineering and Technology (ICISET)* (pp. 157-162). IEEE.

Ojaroudi, N., Ojaroudi, M. and Ghadimi, N., 2012. UWB omnidirectional square monopole antenna for use in circular cylindrical microwave imaging systems. *IEEE Antennas and Wireless Propagation Letters*, *11*, pp.1350-1353.

Ojaroudi, N. and Ghadimi, N., 2015. Omnidirectional microstrip monopole antenna design for use in microwave imaging systems. *Microwave and Optical Technology Letters*, *57*(2), pp.395-401.

Rokunuzzaman, M., Samsuzzaman, M. and Islam, M.T., 2016. Unidirectional wideband 3-D antenna for human head-imaging application. *IEEE Antennas and Wireless Propagation Letters*, *16*, pp.169-172.

Salleh, A., Yang, C.C., Singh, M.S.J. and Islam, M.T., 2019. Development of antipodal Vivaldi antenna for microwave brain stroke imaging system. *Int. J. Eng. Technol*, *8*(3), pp.162-168.

Sohani, B., Khalesi, B., Ghavami, N., Ghavami, M., Dudley, S., Rahmani, A. and Tiberi, G., 2020. Detection of haemorrhagic stroke in simulation and realistic 3-D human head phantom using microwave imaging. *Biomedical Signal Processing and Control*, *61*, p.102001.

Subramanian, S., Sundarambal, B. and Nirmal, D., 2018. Investigation on simulation-based specific absorption rate in ultra-wideband antenna for breast cancer detection. *IEEE sensors journal*, *18*(24), pp.10002-10009.

Talukder, M.S., Samsuzzaman, M., Islam, M.T., Azim, R., Mahmud, M.Z. and Islam, M.T., 2021. Compact ellipse shaped patch with ground slotted broadband monopole patch antenna for head imaging applications. *Chinese Journal of Physics*, *72*, pp.310-326.

Talukder, M.S., Alam, M.M., Islam, M.T., Moniruzzaman, M., Azim, R., Alharbi, A.G., Khan, A.I., Moinuddin, M. and Samsuzzaman, M., 2022. Rectangular slot with inner circular ring patch and partial ground plane based broadband monopole low SAR patch antenna for head imaging applications. *Chinese Journal of Physics*, *77*, pp.250-268.

Wang, L. and Simpkin, R., 2013. Holographic microwave imaging for medical applications. 2013(August), pp.823–833.

Wang, Z., Lim, E.G., Tang, Y. and Leach, M., 2014. Medical applications of microwave imaging. *The Scientific World Journal*, *2014*.

Yoon, Z., Mayank, M. and Stoll, E., 2021. Performance Enhancement Techniques for Patch Antennas of Small Satellites.